



Probing Single-Cell Mechanical Allostasis Using Ultrasound Tweezers

WEIYI QIAN¹ and WEIQIANG CHEN ^{1,2}

¹Department of Mechanical and Aerospace Engineering, New York University, Brooklyn, NY 11201, USA; and ²Department of Biomedical Engineering, New York University, Brooklyn, NY 11201, USA

(Received 11 February 2019; accepted 31 May 2019; published online 13 June 2019)

Associate Editor Stephanie Michelle Willerth oversaw the review of this article.

Abstract

Introduction—In response to external stress, cells alter their morphology, metabolic activity, and functions to mechanically adapt to the dynamic, local environment through cell allostasis. To explore mechanotransduction in cellular allostasis, we applied an integrated micromechanical system that combines an ‘ultrasound tweezers’-based mechanical stressor and a Förster resonance energy transfer (FRET)-based molecular force biosensor, termed “actinin-sstFRET,” to monitor *in situ* single-cell allostasis in response to transient stimulation in real time.

Methods—The ultrasound tweezers utilize 1 Hz, 10-s transient ultrasound pulses to acoustically excite a lipid-encapsulated microbubble, which is bound to the cell membrane, and apply a pico- to nano-Newton range of forces to cells through an RGD-integrin linkage. The actinin-sstFRET molecular sensor, which engages the actin stress fibers in live cells, is used to map real-time actomyosin force dynamics over time. Then, the mechanosensitive behaviors were examined by profiling the dynamics in Ca²⁺ influx, actomyosin cytoskeleton (CSK) activity, and GTPase RhoA signaling to define a single-cell mechanical allostasis.

Results—By subjecting a 1 Hz, 10-s physical stress, single vascular smooth muscle cells (VSMCs) were observed to remodeled themselves in a biphasic mechanical allostatic manner within 30 min that caused them to adjust their

contractility and actomyosin activities. The cellular machinery that underscores the vital role of CSK equilibrium in cellular mechanical allostasis, includes Ca²⁺ influx, remodeling of actomyosin CSK and contraction, and GTPase RhoA signaling. Mechanical allostasis was observed to be compromised in VSMCs from patients with type II diabetes mellitus (T2DM), which could potentiate an allostatic maladaptation.

Conclusions—By integrating tools that simultaneously permit localized mechanical perturbation and map actomyosin forces, we revealed distinct cellular mechanical allostasis profiles in our micromechanical system. Our findings of cell mechanical allostasis and maladaptation provide the potential for mechanophenotyping cells to reveal their pathogenic contexts and their biophysical mediators that underlie multi-etiological diseases such as diabetes, hypertension, or aging.

Keywords—Cellular allostasis, Acoustic tweezers, FRET, Mechanotransduction, Diabetes.

Address correspondence to Weiqiang Chen, Department of Mechanical and Aerospace Engineering, New York University, Brooklyn, NY 11201, USA. Electronic mail: wchen@nyu.edu

Weiqiang Chen is an Assistant Professor in the Departments of Mechanical and Aerospace Engineering and Biomedical Engineering at New York University. He received his B.S. in Physics from Nanjing University and M.S. degrees from Shanghai Jiao Tong University and Purdue University, both in Electrical Engineering. He earned his Ph.D. in Mechanical Engineering from the University of Michigan in 2014. Research in the Chen’s lab focuses on developing new biomaterials, microfluidics, and organ-on-a-chip systems to address emerging biomedical problems in cell mechanobiology, cancer biology, immune engineering, and stem cell-based regenerative medicine. He is the recipient of the American Heart Association Scientist Development Award, the Lab on a Chip Emerging Investigator Award, the New York University Whitehead Fellowship in Biomedical and Biological Sciences, the Goddard Junior Faculty Fellowship, the Baxter Young Investigator Award, the University of Michigan Richard F. & Eleanor A. Towner Prize for Outstanding PhD Research, and the ProQuest Distinguished Dissertation Award.

This article is part of the 2019 Young Innovators issue.



INTRODUCTION

Cells, independently and cooperatively, adapt to changing conditions and stressors through a mechanism, termed ‘allostasis’ that contributes to tissue-level homeostasis.^{55,56} Human system persists physiological regulatory systems such as the nervous, cardiovascular, metabolic or immune systems to protect against

internal and external adverse stimuli, and ultimately better adapt cells to its local environment. Through these critical biological adaptive processes human system can stabilize internal and external subcritical physiological variables to a new steady state to ensure biological functionality. Although allostasis has been widely studied in biology at the organismal level, it has been rarely explored at the single-cell level in the context of mechanical responses.^{25,41,42} At present, it remains unclear how a single cell allostatically adapts to external physical stress in the absence of advanced regulatory systems found at the organismal level. The biophysical responses of cells to dynamic mechanical forces underlies the progression of many diseases and aging. For example, under diseased conditions, vascular cells are unable to adapt to external mechanical stress and, thus, fail to maintain their quiescent phenotype which contributes to the etiology of cardiovascular diseases.⁴⁷ It is widely believed that the effects of mechanical stress on vascular smooth muscle cells (VSMCs) may influence the maintenance of normal vascular contraction and dilation functions and underlie cardiovascular disease progression.^{49,58} However, the cellular contribution to abnormal vascular biomechanics associated with these diseases is not fully understood, and we expect that a disruption in cell allostasis may play a key role in elucidating the biomechanics of vascular disease progression. Therefore, a better understanding of such biomechanical adaptive/maladaptive behaviors, coined cellular ‘mechanical allostasis,’ and its regulatory factors is central to distinguishing the role of allostasis in healthy and disease physiology.

Until now, defining a cell’s “mechanophenotype” has been focusing on measuring mechanical properties of cells, such as stiffness, deformability, and viscoelasticity to distinguish cells in different states.¹⁰ However, even at a steady state, the CSK is highly dynamic, with complex and diverse molecular activities and structural dynamics that results in fluctuations of cell-level properties. In contrast to the extensive study of a cell’s “static” biophysical properties and their relation to cell status, research on how a cell’s dynamic mechanical allostasis in response to mechanical stimuli in diseases are rarely done. Perturbations in a cell’s microenvironment are transient, and CSK structures are highly dynamic. However, determining the variance in time (seconds or minutes) of molecular activities and CSK dynamics under dynamic, transient stresses remains largely unexplored. Dynamic responses to mechanical perturbations predominantly rely on a cell’s CSK integrity and structure. Subtle changes to CSK architecture are associated with pathophysiological conditions that are challenging to distinguish and central to allostatic responses to

mechanical stimuli. We hypothesize that a cell’s mechanical allostasis in response to dynamic mechanical perturbations are “integrators” of a cell’s biophysical properties that can be used to profile a cell’s mechanophenotype in health and disease. Simultaneously, it is paramount to scrutinize the regulatory factors and molecular mechanisms that are responsible for single cell’s mechanical allostasis in responses to transient mechanical perturbation at subcellular and molecular scales.

In response to mechanical forces, a series of mechanosensitive elements must be activated.²⁹ Mechanical forces can activate mechanosensitive ion channels that permit intracellular Ca^{2+} influx, triggering a subsequent activation of regulatory proteins.^{16,27,28,59} For example, Liu *et al.* demonstrated that localized mechanical stress applied by acoustic tweezing cytometry can mediate the opening of mechanosensitive channel of large conductance (MscL) that requires force transduction through the actin CSK.²⁸ The molecular machinery upon Ca^{2+} signaling for controlling cellular contractility relies on intact interactions among actin CSK,⁶ myosin motor activities,⁴⁵ and regulatory proteins, such as GTPase RhoA.^{14,34,51} In response to mechanical perturbations, cells show a dynamic display of contractile forces, yet such observations in mechanical forces and their relays in mechanotransduction vary in the nature of mechanical perturbations and force measurement tools.^{3,9,19,40,66,67} By subjecting cells to mechanical perturbations, single cell contractility has been reported to increase and achieve a higher and more stable contractile state,^{9,12,19,20,61,66,68} while others have reported that cell contractility goes through a rapid excitation and returns to ground states.^{38,40,67} For example, by applying fluid shear stress on human umbilical vein endothelial cells (HUVECs) seeded on a micropillar array, Fu *et al.* reported an instantaneous increase and a gradual decrease to baseline in CSK contractility.³⁸ However, when subjected to mechanical displacements, Fletcher *et al.* demonstrated that single fibroblasts can reach a steady-state contraction force.⁶⁶ Currently, probing cell responses with monophasic adaptation to global,⁶⁶ constant,¹⁵ or frequency-dependent^{21,30,39} mechanical loading on microtissues with a timescale spanning hours are methods commonly reported. In contrast to large-scale organisms, cells function in smaller dimensions and timescales, and cellular allostatic adaptation may occur in seconds or minutes—a much shorter timescale compared to those of the organismal level.³² Moreover, actionable changes in a cell’s microenvironment are transient and dynamic.^{5,17,23,31} Therefore, it is essential to scrutinize the allostatic adaptation of cells in response to localized and transient inputs at the subcellular and molecular scale.

Localized mechanical perturbations to cells using acoustic,^{12,19,20,28,61,68} optical,^{35,63} and magnetic,^{7,13} tweezers systems have been reported to stimulate cells to adjust their CSK and contractility. These methods of applying localized mechanical stress have been shown to modulate multiple cell functions, such as stem cell differentiation^{13,61,68} and survival.¹¹ Among them, acoustic tweezers have emerged as innovative tools for probing cell mechanotransduction due to their ability of applying controllable and localized mechanical forces in high throughput and potential for translational applications, making them ideal tools for studying single cell allostatic behavior. From the perspective of measuring single-cell forces, it is apparent that the events leading to mechanosensitive signaling are mediated by a set of dynamic molecular processes.²⁹ A variety of tools have been developed to probe the mechanical and molecular dynamics in cell mechanotransduction. Among which, Förster resonance energy transfer (FRET)-based biosensors have been highlighted for their capacity of probing subcellular and molecular activities in real time and the compatibility of applications in three dimensional settings. These advantages justify FRET as a great tool for studying the spontaneous and dynamic allostatic behaviors of single cells.⁶⁵ Different types of FRET-based biosensors have been utilized in live cells for reporting biochemical or biophysical dynamics of mechanosensitive proteins in mechanotransduction by mapping the donor-to-acceptor intensity ratio of target molecules to elucidate the subcellular responses to mechanical forces.^{64,65} By integrating the acoustic/ultrasound tweezers with FRET biosensors, we expect that single cell allostasis can be readily investigated.

In this study, we applied an integrated *in vitro* micromechanical system that combines an ultrasound ‘tweezers’ stimulator to apply and modulate transient and localized mechanical forces to single cells and a FRET-based molecular force biosensor to accurately profile *in situ* cell mechanical force dynamics. We observed allostasis in VSMC mechanics when exposed to transient mechanical stress. This mechanical allostasis occurs through a biphasic process: when subjected to a 10-s, transient, local physical stress, cellular mechanics tended to restore to a stable state through a mechanoadaptive process with excited biophysical activity, followed by a decaying adaptive phase. We further found that cellular mechanical allostasis is dependent on the integrity of a mechanosensitive bio-chemo-mechanical feedback, including Ca^{2+} influx, CSK and contraction dynamics, and GTPase RhoA signaling. Disruption of any component in this complex feedback abolished single-cell allostatic behaviors. Compromised mechanical allostatic behaviors were observed from VSMCs from

patients with type II diabetes mellitus (T2DM), which could potentiate an allostatic maladaptation. Our results indicate that dysregulations of mechanical allostasis in cells may be featured in pathological diseases, such as diabetes, hypertension, atherosclerosis, and aging.

MATERIALS AND METHODS

Cell Culture and Reagent

VSMCs were purchased from Lonza and maintained with SmGM-2 Smooth Muscle Growth Medium BulletKit (Lonza). Cells were cultured in the culture medium and maintained at 37 °C with 5% CO_2 . The medium was replaced every 3 days. Passages 3–6 were used in our experiments. Cells were seeded to a glass surface coated with 50 $\mu\text{g}/\text{mL}$ fibronectin (Sigma-Aldrich) at a density of 6000 cells/ cm^2 and incubated overnight before experiments. DNA plasmids PEG-Actinin-M-sstFRET was a gift from Fred Sachs (Addgene plasmid # 61100). Before transfection, VSMCs were seeded onto glass substrates overnight. Cells typically reached 40–60% confluency within 12 h. DNA plasmids were transfected into VSMC using Lipofectamine 2000 (Thermo Fisher Scientific) following protocol previously described.⁸ After being transfected for 24 h, VSMCs were subjected to ultrasound tweezers stimulation. For drug treatment experiments, VSMCs seeded on the glass surface were pretreated with 5 μM Y-27632 (Sigma-Aldrich) or 10 μM blebbistatin (Cayman Chemical) for 1 h before ultrasound tweezers stimulation. Calcium-free experiments were done in Calcium-free medium (Thermo Fisher Scientific).

Single Cell Microbubble Attachment

Before ultrasound tweezers stimulation, VSMCs transfected with Actinin-sstFRET were coated with Targeson microbubbles at a density of 1–2 microbubbles/cell. Essentially, 1 μL of Targosphere® lipid microbubble solution ($3 \times 10^9 \text{ mL}^{-1}$) was mixed with 4 μL of biotinylated Arg-Gly-Asp (RGD) peptide (2 mg/mL, Peptides International) for 20 min at room temperature to prepare the RGD-microbubbles mixture. The RGD-microbubbles mixture was diluted with 100 μL VSMC culture medium. To attach RGD-microbubbles to the cell membrane, cell culture medium was removed from the cell seeded dish, and 30 μL of the diluted RGD-microbubble mixed solution was added to the dish. The dish was flipped over and kept in an incubator for 10 min to allow microbubbles to float and attach to cell membrane. The dish was then washed 3 times with cell culture medium to remove

unbound microbubbles. In our experiments, single cells with only one or two microbubbles attached were selected for ultrasound tweezers stimulation.

Ultrasound Tweezers Stimulation

A 10-MHz ultrasound transducer (V312-SM, Olympus) was used to generate ultrasound pulses to excite microbubbles to apply a transient local force to VSMCs with microbubbles attached. The ultrasound transducer was driven by a function generator (Agilent Technologies 33250A) and a 75 W power amplifier (Amplifier Research 75A250). A pulser/receiver (5072PR, Olympus) and a digital oscilloscope (GW Instek) were used to place the natural focus of the ultrasound transducer at the target surface. The ultrasound transducer was fixed at a 45° angle to horizontal plane, and its working top was submerged in the cell medium 11.25 mm (Rayleigh distance) away from the target cell. Ultrasound pulse was applied at a frequency of 1 Hz.

FRET Measurement

For FRET-based actinin stress sensing, real-time and *in-situ* images of CFP and FRET channels were collected by a microscope (Zeiss observer Z1) and a cooled charge-coupled device (CCD) camera (Hamamatsu Flash 4.0) with two emission filters controlled by a filter changer (480DF40 for CFP and 535DF25 for FRET) using MetaFluor 6.2 software every 30 s for 30 min. The excitation filter set for FRET measurement is ET420/40. The excitation filter set for direct YFP measurement is ET497/16. All filter sets were from Chroma. To obtain satisfactory signal to noise and avoid inducing unnecessary photobleaching, the intensity of the excitation light was controlled by applying 20% transmitted light. To further correct photobleaching that leads to a steady decrease in the FRET ratio over time, the intensity of the FRET channel was multiplied by a correction factor. This correction factor is calculated by dividing the intensity of direct YFP at $t = 0$ by the YFP intensity at a given time point. After the image capture, FRET/CFP ratio was calculated, and the image was processed using a custom-developed MATLAB program (Mathworks) according to the established methods.^{8,46} Basically, the fluorescence intensity of CFP, FRET, and the direct YFP signals on transfected cells were corrected by subtracting the background signals from non-transfected cells. The FRET signals were further corrected by multiplying the correction factor mentioned above. The pixel-by-pixel ratio images of FRET/CFP were calculated based on the corrected fluorescence intensity

images of CFP and FRET to allow quantification and statistical analysis of FRET ratio responses.

Traction Force Measurement Using Micropillar Array

VSMCs were seeded onto micropillar arrays functionalized with fibronectin (50 $\mu\text{g}/\text{mL}$; Sigma-Aldrich) and Alexa-Fluor 647-conjugated fibrinogen (25 $\mu\text{g}/\text{mL}$; Life Technologies) overnight before being subjected to transfection with plasmids PEG-Actinin-M-sstFRET. The processes for the fabrication and functionalization of micropillar have been previously described.^{22,70} Briefly, a silicon master mold with micropost array was fabricated by standard photolithography and deep reactive ion etching (DRIE). A negative PDMS mold with array of holes was then generated through a “casting” process. To generate the PDMS micropillar array, a 1:10 ratio PDMS prepolymer was poured over the negative PDMS mold that was silanized with tridecafluoro-1,1,2,2,-tetrahydrooctyl)-1-trichlorosilane (Sigma-Aldrich) for 4 h under vacuum. Activated cover glass treated with oxygen plasma was then placed on the top of the negative PDMS mold and cured for 40 h in a 110 °C oven. Cover glass with PDMS micropillar was then peeled off from the PDMS negative mold. The collapsed micropillar array was sonicated in 100% ethanol and dried using a critical point dryer (Samdri-PVT-3D, Tousimis). Microcontact printing was used to modify the PDMS micropillar top with fibronectin for cell attachment and Alexa-Fluor 647-conjugated fibrinogen for pillar visualization. After 24 h of transfection, VSMCs were starved for 3 h and then treated with either 20 μM LPA or 10 μM Y-27632 in cell culture medium without serum. Deflection of the micropillar was monitored for 30 min at an interval of 30 s by taking the fluorescent Alexa-Fluor 647 images of the micropillar tip. Quantitative analysis of cellular CSK tension was performed by quantifying the deflection of micropillar using a custom-developed MATLAB program (Mathworks).⁶⁷ For actinin stress sensing, real-time and *in-situ* images of CFP and FRET channels with two emission filters controlled by a filter changer (480DF40 for CFP and 535DF25 for FRET) were collected together with the deflections of micropillars.

Statistical Analysis

Quantitative results in this study were reported as mean \pm SE. Statistical significance was tested by using Student's *t* test, where null hypothesis was rejected at $p < 0.05$.

RESULTS

Integrated Ultrasound Tweezers and FRET Sensor System for Probing Cellular Mechanical Responses

We applied an integrated micromechanical system composed of an ultrasound ‘tweezers’ mechanical stress stimulator and a FRET-based molecular force biosensor to monitor *in situ* cell dynamic response in real time to a transient mechanical stimulation (Fig. 1). Specifically, the ultrasound tweezers utilized an ultrasound transducer to apply a 10 s, 1 Hz, ~ 100 pN of transient and local mechanical force to cells *via* RGD-integrin binding of a microbubble bound to the cell membrane (Fig. 1a); The actinin-sstFRET biosensor^{43,52} was applied to track the molecular tension across the actin filament during allostatic remodeling (Fig. 1b). As shown in Fig. 1c and Supplementary Video 1, during ultrasound stimulation, microbubbles attached to the cell membrane exhibited periodically translational displacements relative to their original location. This microbubble displacement-induced mechanical stress to cells could activate ion channels on the cell membrane and trigger mechanotransduction in the cell cytoskeleton. To verify that the actinin-

sstFRET biosensor can report intracellular tension dynamics, we applied biochemical perturbations and used the micropillar array cellular force sensor to measure cell traction force together with the actinin-sstFRET biosensor. The micropillar array has been broadly applied in measuring cell traction force dynamics in cell migration,¹⁸ differentiation,²² and development⁶⁹ with spatial and temporal accuracy. VSMCs seeded on micropillar array and transfected with actinin-sstFRET biosensor were either treated with 20 μ M lysophosphatidic acid (LPA), which activates RhoA and increases cell contractility,^{36,71} or treated with 10 μ M Y-27632, a ROCK inhibitor that decreases cell contractility.⁴ As shown in Fig. 2, VSMCs treated with LPA showed a continuous increase in traction force within 30 min as measured by micropillar array (Figs. 2a and 2b). At the same time, the FRET ratio of the actinin-sstFRET biosensor continuously decreased as expected. When treated with Y-27632, cell contractility decreased, and the FRET ratio increased within the 30 min during the measurement period (Figs. 2c and 2d). These experiments confirmed that the distance-based actinin-sstFRET

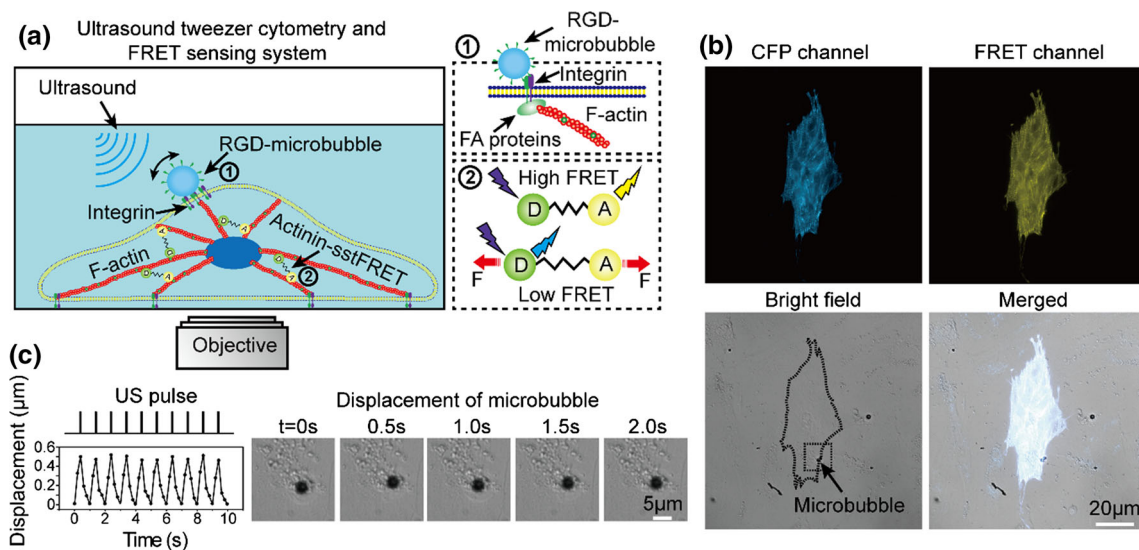


FIGURE 1. Integrated ultrasound tweezers and FRET sensing system. (a) A schematic showing ultrasound excitation of microbubbles attached *via* RGD-integrin binding to the membrane of a cell. Ultrasound was applied 45° with respect to the vertical direction in plane. Inset figure shows microbubble functionalized with RGD binding to cell integrin and is connected to F-actin of CSK; inset figure shows the principle of the distance-based actin-sstFRET intracellular force sensor. Intracellular force dynamics will lead to the change of the donor-acceptor distance, and thus the FRET ratio. A lower FRET ratio indicates larger force, and a higher FRET ratio indicates lower force. (b) Representative images showing a VSMC transfected with actin-sstFRET sensor and imaged in CFP and FRET channels. Bright field image shows microbubble attached to this VSMC. (c) Line plot and brightfield images showing the temporal evolution of the lateral displacement of the single bubble attached to the VSMC in (b) within 10 s.

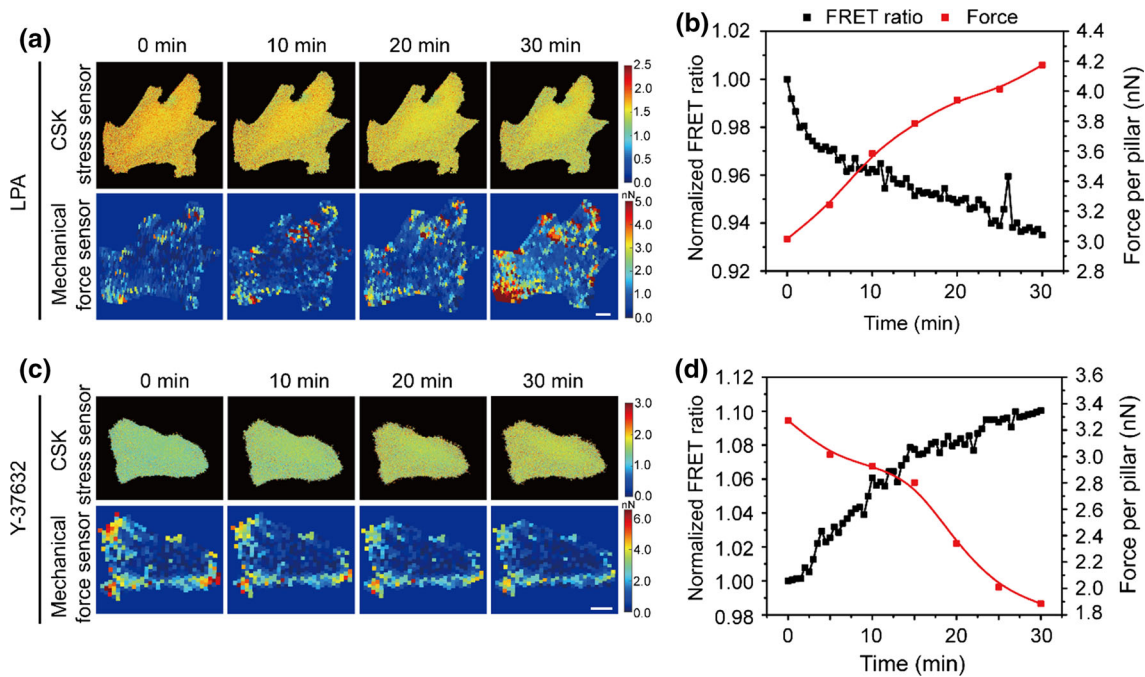


FIGURE 2. Validation of the actinin-sstFRET sensor in measuring cell intracellular force with micropillar array. (a) Images show the temporal evolution of forces of a representative VSMC upon treated with 20 μM LPA measured by actinin-sstFRET sensor and micropillar array. (b) Quantified evolution of the FRET ratio and traction force measured by micropillar array. Upon treated with 20 μM LPA, cell contractility continuously increased while the FRET ratio continuously decreased. (c) Images show the temporal evolution of forces of a representative VSMC upon treated with 10 μM Y-27632 measured by actinin-sstFRET sensor and micropillar array. (d) Quantified evolution of the FRET ratio and traction force measured by micropillar array. Upon treated with 10 μM Y-27632, cell contractility continuously decreased while the FRET ratio continuously increased. Scale bar: 20 μm .

biosensor can accurately report intercellular tension dynamics.

Allostatic Response of Cells to Ultrasound Tweezers Stimulation

Using our integrated micromechanical system, we then investigated how cells would mechanically respond to the transient mechanical stress. We locally applied a 10 s, 1 Hz, ~ 100 pN mechanical force to cells *via* RGD-integrin binding of a microbubble bound to the cell membrane and, initially, examined Ca^{2+} influx upon ultrasound tweezers stimulation. We observed that Fluo-4 calcium sensor intensity presented a rapid rise of cytosolic Ca^{2+} during adaptation (Fig. 3a and Supplementary Video 2), suggesting that a transient Ca^{2+} influx happens simultaneously with the transient mechanical stress. We expected that actomyosin CSK tension would be activated by the transient mechanical stress-induced transient Ca^{2+} influx. Indeed, we observed that cells actively modulated intracellular tension (Figs. 3b and 3c) in response to a transient 10 s mechanical stress. Generally, the appearance of mechanical allostasis is identified by an increase in intracellular tension (decrease in FRET ratio) in the first 5 min after stimulation followed by a

monotonical decrease to the initial ground-state value (Figs. 3b and 3c). However, for cells without bubble attachment, we observed no significant change in CSK force (Figs. 3b and 3c). In conclusion, this mechanical analysis demonstrated that cells followed a biphasic allostastic adaptation process when acted upon by a transient and local stimulation. Cell mechanics (CSK tension) were first elevated in an acute excited phase ($t = 0-5$ min) and then decayed to the initial mechanobiological ground state in an adaptation phase ($t = 5-30$ min).

Cellular Mechanical Allostasis is Dependent on the Integrity of a Bio-chemo-mechanical Contraction Model

In response to the Ca^{2+} influx through ion channels activated by the transient and localized mechanical stimulation, VSMCs demonstrated cell allostastic behavior by modulating CSK contraction. A bio-chemo-mechanical model combined with Rho/ROCK regulation can be coined to explain this contraction dynamics³³ (Fig. 4a). Upon Ca^{2+} influx, myosin light-chain kinase (MLCK) is activated by a calmodulin-mediated mechanism. Activated MLCK further promotes the phosphorylation of myosin light chains and

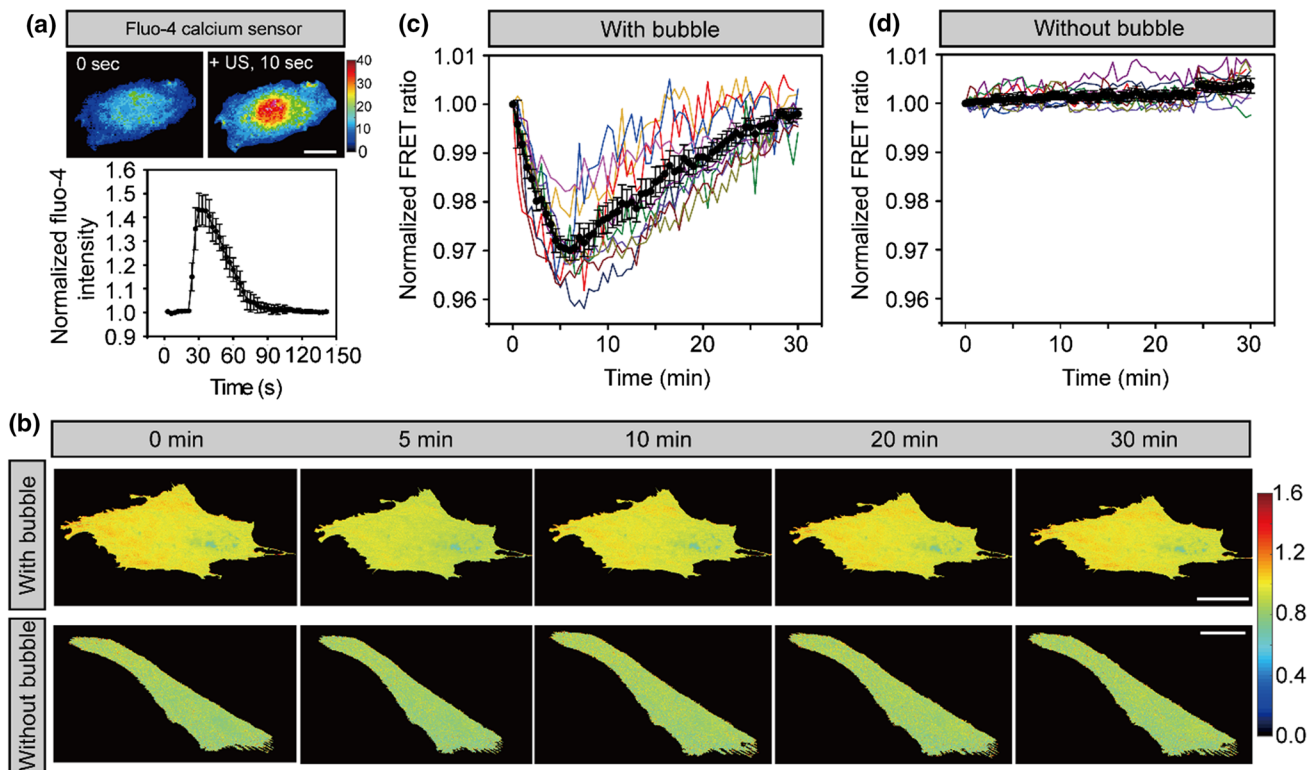


FIGURE 3. Single cell mechanical allostasis. (a) The time course of the normalized Fluo-4 calcium sensor intensity change in VSMCs before and after 10 s of ultrasound tweezers stimulation ($n = 10$). (b) Representative temporal evolution of FRET/CFP ratio images of the actinin-sstFRET sensor in VSMCs functionalized with microbubble (top panel) and VSMCs without functionalization of microbubble (bottom panel) before ($t = 0$ min) and after subjected to 10-s US stimulation at 5, 10, 20, and 30 min respectively. (c) and (d) Quantified temporal evolutions of the FRET/CFP ratio during single VSMCs mechanical response to a 10-s mechanical stress for VSMCs functionalized with microbubble (c) and VSMCs without functionalization of microbubble (d). In (a), (c) and (d), traces of different color refer to individual cells and solid black dots represents the mean \pm error with $n = 10$. Scale bar in (a) and (b): 20 μm .

contributes to the binding of myosin to F-actin bundles following CSK tension dynamics. Meanwhile, inhibiting the dephosphorylation of myosin light chains by GTPase Rho/ROCK is equally important to modulating CSK tension dynamics. Thus, we hypothesize that the integrity of this bio-chemo-mechanical feedback system, including Ca^{2+} influx, Rho/ROCK signaling, and myosin contraction, plays a vital role in regulating cell allostasis, and a disruption of any component in this cycle may be demonstrated by impaired cell allostatic behavior and implicated in pathological conditions such as diabetes.

We therefore used our micromechanical system to study the effect of the proposed bio-chemo-mechanical feedback on regulating cell allostatic behaviors. We used three conditions to individually study the effect of each component in the bio-chemo-mechanical feedback system: Ca^{2+} -free medium, which excludes the influx of Ca^{2+} into cells upon ultrasound tweezers stimulation; Y-27632, which inhibits the activity of Rho/ROCK;⁴ and blebbistatin, which inhibits myosin motor activity and, thus, affects the CSK tension

dynamics.² As shown in Figs. 4b and 4c, inhibiting activities of Rho/ROCK and myosin did not alter the influx of Ca^{2+} into VSMCs pretreated with Y-27632 and blebbistatin upon ultrasound tweezers stimulation. However, in Ca^{2+} -free medium, an influx of Ca^{2+} was not observed. Correspondingly, allostatic behavior was not observed for VSMCs in Ca^{2+} -free medium (Fig. 4d), confirming that the mechanosensitive Ca^{2+} signaling triggers cell allostasis. For normal VSMCs pretreated with Y-27632, they demonstrated compromised allostatic behavior (Fig. 4e). The maximum change of actinin-sstFRET ratio of VSMCs treated with Y-27632 is about one third of that in normal VSMCs at the peak time in cell allostasis dynamics. These results confirmed that the Rho/ROCK activity is critical to cell allostasis dynamics. Similarly, directly inhibiting myosin motor activity largely abolished cell allostasis (Fig. 4f). Overall, in response to inhibitor perturbations, cell allostatic behaviors were observed to be compromised, confirming the importance of the integrity of the proposed bio-chemo-mechanical feedback system in regulating cell allostasis.

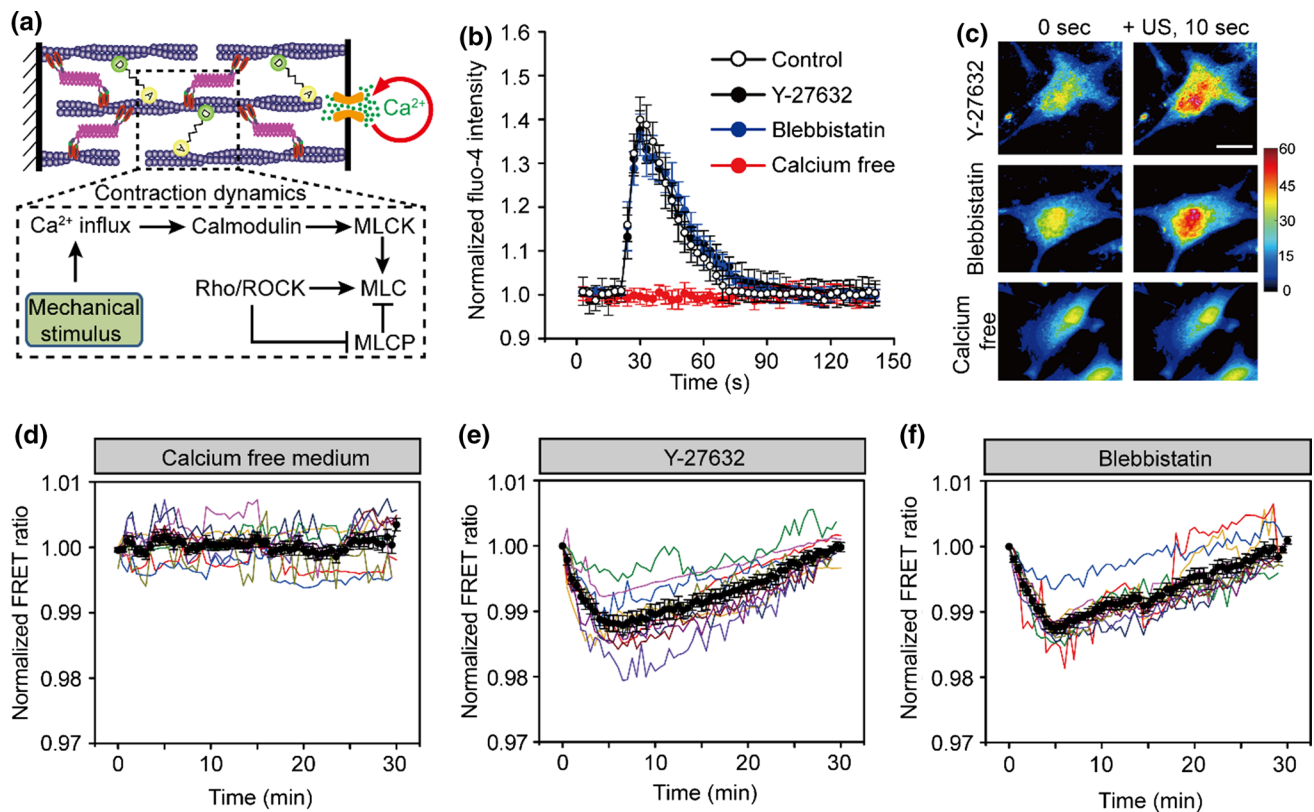


FIGURE 4. Single cell allostasis relies on the integrity of a bio-chemo-mechanical feedback. (a) Schematic showing a proposed bio-chemo-mechanical model describing the signaling network in cell allostasis. (b) The time course of the normalized Fluo-4 calcium sensor intensity change in VSMCs upon ultrasound tweezers stimulation under different conditions as indicated ($n = 10$). (c) Representative heatmap images of VSMCs pretreated with Y-27632 or blebbistatin, and in Ca^{2+} -free medium with Fluo-4 calcium sensor before and after 10 s of ultrasound tweezers stimulation. (d)–(f) Quantified temporal evolutions of the FRET/CFP ratio during single VSMCs mechanical response to a 10-s mechanical stress for VSMCs in Ca^{2+} -free medium (d) or pretreated with Y-27632 (e) or blebbistatin (f). In (b), data represents the mean \pm error with $n = 10$; in (d)–(f), traces of different color refer to individual cells and solid black dots represents the mean \pm error with $n = 10$. Scale bar in (c): 20 μ m.

Cellular Mechanical Allostasis is Featured in Pathological Conditions

Cellular mechanical allostasis, which relies on the interplay of the Ca^{2+} signaling, Rho/ROCK activity, and myosin motor contraction in this bio-chemo-mechanical feedback, represents the response of cells to mechanical cues. Dysregulation of such responses, which may come from the dysregulation of any component in the bio-chemo-mechanical feedback system, may be featured in pathophysiological conditions such as cardiovascular diseases.^{24,44,53,62} For instance, one study found that depletion of ion channels on VSMCs, which inhibit stretch-induced Ca^{2+} signaling in cells' cytoplasm, impairs arterial remodeling in response to hypertension.⁵³ Recent studies revealed that the expression and activity of GTPase RhoA was lower in SMCs isolated from patients with T2DM than those from age-matched control groups,⁵⁴ and patients with T2DM are usually prone to additional cardiovascular diseases.⁴⁸ In light of these findings, we hypothesize that cell allostatic behaviors, which highly rely on the

integrity of the aforementioned cell contraction model, can reflect cell biophysical phenotypes that bear pathological tendencies in diseases. As an example, we used VSMCs isolated from patients with T2DM for cell allostatic analysis. We firstly examined the Ca^{2+} signaling triggered by the ultrasound tweezers. T2DM-VSMCs demonstrated indistinguishable Ca^{2+} influx behavior compared to normal VSMCs (Fig. 5a). However, the allostatic behaviors of VSMCs from patients with T2DM demonstrated a time delay in achieving the maximum CSK tension, from ~ 5 min in normal VSMCs to ~ 10 min in T2DM-VSMCs (Figs. 5b and 5c). In addition, there was a significant difference in the magnitude of the maximum CSK tension achieved between normal VSMCs and T2DM-VSMCs, with $3.14\% \pm 0.26\%$ for normal VSMCs and $2.15\% \pm 0.15\%$ for T2DM-VSMCs. These altered characteristics of allostatic behaviors between normal and T2DM-VSMCs imply differences in their bio-chemo-mechanical force generation processes,⁴⁴ and the altered expression and activity of GTPase RhoA as

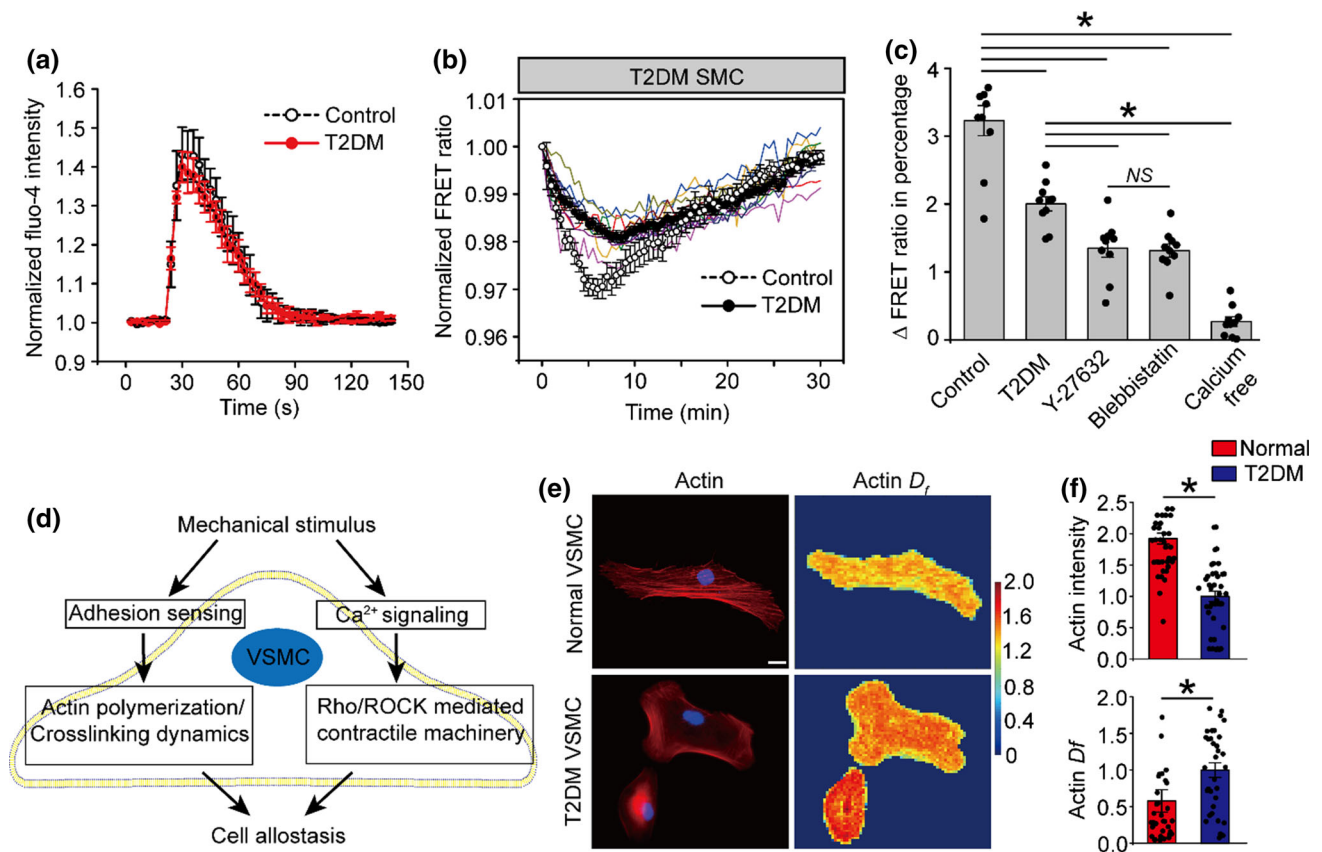


FIGURE 5. Single cell mechanical allostasis in T2DM-VSMCs. (a) The time course of the normalized Fluo-4 calcium sensor intensity change in VSMCs from patients with T2DM upon ultrasound tweezers stimulation. Control data is plotted in hollow dot for comparison. ($n = 10$). (b) Quantified temporal evolutions of the FRET/CFP ratio during single T2DM-VSMCs mechanical response to a 10-s mechanical stress. Control data is plotted in hollow dot for comparison. (c) Bar plot shows the quantified maximum change of FRET/CFP ratio in the allostastic dynamics for normal VSMCs, T2DM-VSMCs, and VSMCs pretreated with Y-27632, blebbistatin or in Ca^{2+} -free medium. (d) A schematic illustrating that Ca^{2+} -triggered and Rho/ROCK-mediated myosin motor contraction, as well as CSK events like actin polymerization and crosslinking, contribute to VSMC allostasis and may be altered in diseases like diabetes. (e) Representative fluorescent images and corresponding fractal dimensions (D_f) of F-actin filaments in normal VSMC and T2DM-VSMC. (f) Quantified intensity and D_f of F-actin in normal VSMCs and T2DM-VSMCs. The quantitative analysis of F-actin filaments indicates that T2DM-VSMC has a lower level of actin and higher D_f of actin, suggesting a more diffused pattern of F-actin filaments in cells. In (a), data represents the mean \pm error with $n = 10$; In (b), traces of different color refer to individual T2DM VSMCs and solid black dots with error bar represents the mean \pm error with $n = 10$. In (c) and (f), p values were calculated using the Student's unpaired sample t test. $*p < 0.05$. Scale bar in (e): 20 μm .

suggested by the previous study⁵⁴ may be responsible for these changes.

While we demonstrated that MLC phosphorylation, which is initiated by Ca^{2+} signaling and mediated by Rho/ROCK, is critical for our observed VSMC allostasis, we did not consider the effect of actin polymerization and crosslinking dynamics in generating tension in the discussed bio-chemo-mechanical model. In fact, when cells adapt to mechanical forces, the dynamic polymerization of G-actin to F-actin, F-actin crosslinking, and adhesion assembly play important roles when engaging with contractile myosin for generating force²⁶ (Fig. 5d). Therefore, it is possible that the different allostastic behaviors between normal and T2DM-VSMCs may be also caused by these CSK events. When analyzing CSK structures by

immunostaining F-actin in normal and T2DM-VSMCs, we found that T2DM-VSMCs showed low-density and branched F-actin characteristics, compared to the high-density and aligned F-actin structures in normal VSMCs (Figs. 5e and 5f). Moreover, we quantified the actin structures in both cell types using actin fractal dimensions (D_f), which describes complex patterns of F-actin filaments in cells.¹ As shown in Figs. 5e and 5f, there is a distinct difference in distribution (D_f) of F-actin filaments in VSMCs and T2DM-VSMCs with a significantly larger D_f value in T2DM-VSMCs, indicating a more chaotic F-actin structure and a distinct mechanophenotype in T2DM-VSMCs. When considering cell force generation models that include these CSK events, it may still be true that cell allostastic behaviors would be different in

pathological conditions. Therefore, our findings provide a method for distinguishing cells' phenotypes by mapping cellular allostasis.

DISCUSSION

In the present study, we applied an integrated ultrasound tweezers perturbation and FRET sensing system to study spontaneous cellular allostatic behaviors and explored the bio-chemo-mechanical model that governs the generation of forces by VSMCs in response to localized mechanical stress. We further demonstrated the possibility of profiling the dynamics of a cell's mechanical allostasis for cell mechanophenotyping based on cell's intrinsic actomyosin CSK property changes.

Cells actively modulate cellular sensing and signaling transduction components, such as cell CSK structures and intra- and inter-cellular mechanosensitive molecules to adapt to mechanical cues.^{37,50,57,60,72} Yet it remains unclear how the transformation or deterioration of a cell's CSK properties featured in disease progression contributes to a cell's dynamics response to mechanical stress in allostasis. As a cell makes up the foundation of larger-scale behaviors, exploring single-cell allostasis at a subcellular domain may help us better understand the etiology of various diseases and progression of aging. Using our micromechanical system, we successfully mapped VSMCs' mechanical allostasis. Single VSMCs demonstrated their allostatic behaviors by actively modulating their intracellular tension and showed an increase in CSK tension in the first 5 min after stimulation and then a monotonic decrease to the initial ground-state value with 30 min. *In vivo*, SMCs are arranged circumferentially into multiple layers and respond to dynamic blood flow stress to maintain the integrity of arteries. Our observed allostatic behaviors of VSMCs imply that in response to mechanical perturbations, VSMCs hold the ability to respond and recover from external stress, performing robust allostatic behaviors for achieving steady state.

We further identified that cellular allostasis is dependent on the integrity of a bio-chemo-mechanical feedback that controls VSMC contraction. Actomyosin cross-bridge cycling has been previously identified as the mechanism for tension development in SMCs. Loss of a contractile SMC phenotype from human genetic variation has resulted in progressive aortic enlargement and dissection, emphasizing the importance of healthy cellular allostasis in maintaining tissue integrity. In our study, we found that disruption

of any component in the bio-chemo-mechanical feedback results in an allostatic maladaptation. Studies on the phenotypes of SMCs from normal and T2DM patients of the same age have revealed that Rho/ROCK activity is compromised in T2DM SMCs. Our study also found that T2DM SMCs demonstrated a compromised allostasis. This compromised allostasis in T2DM SMCs may also arise from other factors such as a distinct CSK structures compare to normal SMCs.

Our integrated ultrasound tweezers perturbation and FRET sensing system can be readily applied to study both single and multi-cell level allostatic behaviors. With the assistance of microbubble agents, the acoustic tweezers can deliver transient and localized mechanical perturbations to either a single-cell or cell-colony system. In addition, the functions of other force transmission molecular such as actin-crosslinking protein filamin and adhesion protein talin can be readily explored with the integration of corresponding FRET-based molecular sensors. The versatility of the FRET molecular sensors combined with acoustic tweezers can further enable a detailed mechanistic study of cellular allostasis. Theoretic modeling of cell allostasis from molecular mechanism studies can further be derived to predict cell mechanical allostasis in various pathological conditions.

Altogether, we demonstrated here the concept of cellular mechanical allostasis and profiling its dynamics as a diagnostic tool for cell mechanophenotyping as observed with T2DM SMCs and their unique allostatic maladaptation. Our system can be easily extended to other diseases involving cellular damage and tissue dysfunction. For example, aging is a temporal process involving progressive functional decline of cell/tissue. Our successful mapping VSMC allostasis offers proof of concept that this method can predict the adaptation or maladaptation for young *vs.* aged cells and provides an alternative approach to use cellular 'allostatic phenotype' to explore biophysical mechanisms of the aging processes. It may even be interesting to apply our analysis to determine cellular aging which may be associated with age-related cell biophysical changes. Finally, key molecular mechanisms that may lead to the transformation of healthy mechanical allostasis into an allostatic maladaptation through alterations in mechanotransduction in cell aging can also be explored.

ELECTRONIC SUPPLEMENTARY MATERIAL

The online version of this article (<https://doi.org/10.1007/s12195-019-00578-z>) contains supplementary material, which is available to authorized users.

ACKNOWLEDGMENTS

We acknowledge financial support from the Department of Mechanical and Aerospace Engineering at New York University, the American Heart Association Scientist Development Grant (16SDG31020038), the National Science Foundation (CBET 1701322), and the National Institute of Health (R21EB025406).

CONFLICT OF INTEREST

Weiyi Qian and Weiqiang Chen declare that they have no conflicts of interest.

ETHICAL APPROVAL

This study does not involve any human studies and animal studies by any author in this article.

REFERENCES

- ¹Alhussein, G., A. Shanti, I. A. Farhat, S. B. Timraz, N. S. Alwahaab, Y. E. Pearson, M. N. Martin, N. Christoforou, and J. C. Teo. A spatiotemporal characterization method for the dynamic cytoskeleton. *Cytoskeleton* 73:221–232, 2016.
- ²Allingham, J. S., R. Smith, and I. Rayment. The structural basis of blebbistatin inhibition and specificity for myosin II. *Nat. Struct. Mol. Biol.* 12:378, 2005.
- ³Balasubramanian, L., C.-M. Lo, J. S. Sham, and K.-P. Yip. Remanent cell traction force in renal vascular smooth muscle cells induced by integrin-mediated mechanotransduction. *Am. J. Physiol. Cell Physiol.* 304:C382–C391, 2013.
- ⁴Beningo, K. A., K. Hamao, M. Dembo, Y.-L. Wang, and H. Hosoya. Traction forces of fibroblasts are regulated by the Rho-dependent kinase but not by the myosin light chain kinase. *Arch. Biochem. Biophys.* 456:224–231, 2006.
- ⁵Binnewies, M., E. W. Roberts, K. Kersten, V. Chan, D. F. Fearon, M. Merad, L. M. Coussens, D. I. Gabrilovich, S. Ostrand-Rosenberg, and C. C. Hedrick. Understanding the tumor immune microenvironment (TIME) for effective therapy. *Nat. Med.* 24:541–550, 2018.
- ⁶Blanchoin, L., R. Boujemaa-Paterski, C. Sykes, and J. Plastino. Actin dynamics, architecture, and mechanics in cell motility. *Physiol. Rev.* 94:235–263, 2014.
- ⁷Bonakdar, N., R. Gerum, M. Kuhn, M. Spörrer, A. Lipfert, W. Schneider, K. E. Aifantis, and B. Fabry. Mechanical plasticity of cells. *Nat. Mater.* 15:1090, 2016.
- ⁸Broussard, J. A., B. Rappaz, D. J. Webb, and C. M. Brown. Fluorescence resonance energy transfer microscopy as demonstrated by measuring the activation of the serine/threonine kinase Akt. *Nat. Protoc.* 8:265, 2013.
- ⁹Brown, R., R. Prajapati, D. McGrouther, I. Yannas, and M. Eastwood. Tensional homeostasis in dermal fibroblasts: Mechanical responses to mechanical loading in three-dimensional substrates. *J. Cell. Physiol.* 175:323–332, 1998.
- ¹⁰Chen, W., S. G. Allen, W. Qian, Z. Peng, S. Han, X. Li, Y. Sun, C. Fournier, L. Bao, and R. H. Lam. Biophysical phenotyping and modulation of ALDH + inflammatory breast cancer stem-like cells. *Small* 15:1802891, 2019.
- ¹¹Chen, D., Y. Sun, C. X. Deng, and J. Fu. Improving survival of disassociated human embryonic stem cells by mechanical stimulation using acoustic tweezing cytometry. *Biophys. J.* 108:1315–1317, 2015.
- ¹²Chen, D., Y. Sun, M. S. Gudur, Y.-S. Hsiao, Z. Wu, J. Fu, and C. X. Deng. Two-bubble acoustic tweezing cytometry for biomechanical probing and stimulation of cells. *Biophys. J.* 108:32–42, 2015.
- ¹³Chowdhury, F., S. Na, D. Li, Y.-C. Poh, T. S. Tanaka, F. Wang, and N. Wang. Material properties of the cell dictate stress-induced spreading and differentiation in embryonic stem cells. *Nat. Mater.* 9:82, 2010.
- ¹⁴Chrzanowska-Wodnicka, M., and K. Burridge. Rho-stimulated contractility drives the formation of stress fibers and focal adhesions. *J. Cell Biol.* 133:1403–1415, 1996.
- ¹⁵Collinsworth, A. M., C. E. Torgan, S. N. Nagda, R. J. Rajalingam, W. E. Kraus, and G. A. Truskey. Orientation and length of mammalian skeletal myocytes in response to a unidirectional stretch. *Cell Tissue Res.* 302:243–251, 2000.
- ¹⁶Coste, B., B. Xiao, J. S. Santos, R. Syeda, J. Grandl, K. S. Spencer, S. E. Kim, M. Schmidt, J. Mathur, and A. E. Dubin. Piezo proteins are pore-forming subunits of mechanically activated channels. *Nature* 483:176, 2012.
- ¹⁷Dietzel, I., and U. Heinemann. Dynamic variations of the brain cell microenvironment in relation to neuronal hyperactivity. *Ann. N. Y. Acad. Sci.* 481:72–84, 1986.
- ¹⁸Du Roure, O., A. Saez, A. Buguin, R. H. Austin, P. Chavrier, P. Siberzan, and B. Ladoux. Force mapping in epithelial cell migration. *Proc. Natl. Acad. Sci. USA* 102:2390–2395, 2005.
- ¹⁹Fan, Z., Y. Sun, D. Chen, D. Tay, W. Chen, C. X. Deng, and J. Fu. Acoustic tweezing cytometry for live-cell subcellular modulation of intracellular cytoskeleton contractility. *Sci. Rep.* 3:2176, 2013.
- ²⁰Fan, Z., X. Xue, R. Perera, S. Nasr Esfahani, A. A. Exner, J. Fu, and C. X. Deng. Acoustic actuation of integrin-bound microbubbles for mechanical phenotyping during differentiation and morphogenesis of human embryonic stem cells. *Small* 14:1803137, 2018.
- ²¹Faust, U., N. Hampe, W. Rubner, N. Kirchgessner, S. Safran, B. Hoffmann, and R. Merkel. Cyclic stress at mHz frequencies aligns fibroblasts in direction of zero strain. *PLoS ONE* 6:e28963, 2011.
- ²²Fu, J., Y.-K. Wang, M. T. Yang, R. A. Desai, X. Yu, Z. Liu, and C. S. Chen. Mechanical regulation of cell function with geometrically modulated elastomeric substrates. *Nat. Methods* 7:733, 2010.
- ²³Gattazzo, F., A. Urciuolo, and P. Bonaldo. Extracellular matrix: a dynamic microenvironment for stem cell niche. *Biochim. Biophys. Acta* 2506–2519:2014, 1840.
- ²⁴Ghigo, A., M. Laffargue, M. Li, and E. Hirsch. PI3 K and calcium signaling in cardiovascular disease. *Circ. Res.* 121:282–292, 2017.
- ²⁵Goldstein, D. S., and B. McEwen. Allostasis, homeostats, and the nature of stress. *Stress* 5:55–58, 2002.
- ²⁶Gunst, S. J., and W. Zhang. Actin cytoskeletal dynamics in smooth muscle: a new paradigm for the regulation of smooth muscle contraction. *Am. J. Physiol. Cell Physiol.* 295:C576–C587, 2008.

- ²⁷Hayakawa, K., H. Tatsumi, and M. Sokabe. Actin stress fibers transmit and focus force to activate mechanosensitive channels. *J. Cell Sci.* 121:496–503, 2008.
- ²⁸Heureaux, J., D. Chen, V. L. Murray, C. X. Deng, and A. P. Liu. Activation of a bacterial mechanosensitive channel in mammalian cells by cytoskeletal stress. *Cell. Mol. Bioeng.* 7:307–319, 2014.
- ²⁹Hoffman, B. D., C. Grashoff, and M. A. Schwartz. Dynamic molecular processes mediate cellular mechanotransduction. *Nature* 475:316, 2011.
- ³⁰Hsu, H.-J., C.-F. Lee, and R. Kaunas. A dynamic stochastic model of frequency-dependent stress fiber alignment induced by cyclic stretch. *PLoS ONE* 4:e4853, 2009.
- ³¹Humphrey, J. D., E. R. Dufresne, and M. A. Schwartz. Mechanotransduction and extracellular matrix homeostasis. *Nat. Rev. Mol. Cell Biol.* 15:802, 2014.
- ³²Kaksonen, M., C. P. Torek, and D. G. Drubin. A modular design for the clathrin-and actin-mediated endocytosis machinery. *Cell* 123:305–320, 2005.
- ³³Kato, S., T. Osa, and T. Ogasawara. Kinetic model for isometric contraction in smooth muscle on the basis of myosin phosphorylation hypothesis. *Biophys. J.* 46:35, 1984.
- ³⁴Kaunas, R., P. Nguyen, S. Usami, and S. Chien. Cooperative effects of Rho and mechanical stretch on stress fiber organization. *Proc. Natl. Acad. Sci. USA* 102:15895–15900, 2005.
- ³⁵Kim, T.-J., C. Joo, J. Seong, R. Vafabakhsh, E. L. Botvinick, M. W. Berns, A. E. Palmer, N. Wang, T. Ha, and E. Jakobsson. Distinct mechanisms regulating mechanical force-induced Ca^{2+} signals at the plasma membrane and the ER in human MSCs. *Elife* 4:e04876, 2015.
- ³⁶Kranenburg, O., M. Poland, M. Gebbink, L. Oomen, and W. H. Moolenaar. Dissociation of LPA-induced cytoskeletal contraction from stress fiber formation by differential localization of RhoA. *J. Cell Sci.* 110:2417–2427, 1997.
- ³⁷Labernadie, A., T. Kato, A. Brugués, X. Serra-Picamal, S. Derzsi, E. Arwert, A. Weston, V. González-Tarragó, A. Elosegui-Artola, and L. Albertazzi. A mechanically active heterotypic E-cadherin/N-cadherin adhesion enables fibroblasts to drive cancer cell invasion. *Nat. Cell Biol.* 19:224, 2017.
- ³⁸Lam, R. H., Y. Sun, W. Chen, and J. Fu. Elastomeric microposts integrated into microfluidics for flow-mediated endothelial mechanotransduction analysis. *Lab Chip* 12:1865–1873, 2012.
- ³⁹Livne, A., E. Bouchbinder, and B. Geiger. Cell reorientation under cyclic stretching. *Nat. Commun.* 5:3938, 2014.
- ⁴⁰Mann, J. M., R. H. Lam, S. Weng, Y. Sun, and J. Fu. A silicone-based stretchable micropost array membrane for monitoring live-cell subcellular cytoskeletal response. *Lab Chip* 12:731–740, 2012.
- ⁴¹McEwen, B. S. Stress, adaptation, and disease: allostasis and allostatic load. *Ann. N. Y. Acad. Sci.* 840:33–44, 1998.
- ⁴²McEwen, B. S., and J. C. Wingfield. The concept of allostasis in biology and biomedicine. *Horm. Behav.* 43:2–15, 2003.
- ⁴³Meng, F., and F. Sachs. Visualizing dynamic cytoplasmic forces with a compliance-matched FRET sensor. *J. Cell Sci.* 124:261–269, 2011.
- ⁴⁴Milewicz, D. M., K. M. Trybus, D.-C. Guo, H. L. Sweeney, E. Regalado, K. Kamm, and J. T. Stull. Altered smooth muscle cell force generation as a driver of thoracic aortic aneurysms and dissections. *Arterioscler. Thromb. Vasc. Biol.* 37:26–34, 2017.
- ⁴⁵Murrell, M., P. W. Oakes, M. Lenz, and M. L. Gardel. Forcing cells into shape: the mechanics of actomyosin contractility. *Nat. Rev. Mol. Cell Biol.* 16:486, 2015.
- ⁴⁶Palmer, A. E., and R. Y. Tsien. Measuring calcium signaling using genetically targetable fluorescent indicators. *Nat. Protoc.* 1:1057, 2006.
- ⁴⁷Pasterkamp, G., D. P. de Kleijn, and C. Borst. Arterial remodeling in atherosclerosis, restenosis and after alteration of blood flow: potential mechanisms and clinical implications. *Cardiovasc. Res.* 45:843–852, 2000.
- ⁴⁸Porter, K. E., and K. Riches. The vascular smooth muscle cell: a therapeutic target in type 2 diabetes? *Clin. Sci.* 125:167–182, 2013.
- ⁴⁹Pyle, A. L., and P. P. Young. Atheromas feel the pressure: biomechanical stress and atherosclerosis. *Am. J. Pathol.* 177:4–9, 2010.
- ⁵⁰Qian, W., L. Gong, X. Cui, Z. Zhang, A. Bajpai, C. Liu, A. B. Castillo, J. C. Teo, and W. Chen. Nanotopographic regulation of human mesenchymal stem cell osteogenesis. *ACS Appl. Mater. Interfaces.* 9:41794–41806, 2017.
- ⁵¹Raftopoulos, M., and A. Hall. Cell migration: Rho GTPases lead the way. *Dev. Biol.* 265:23–32, 2004.
- ⁵²Rahimzadeh, J., F. Meng, F. Sachs, J. Wang, D. Verma, and S. Z. Hua. Real-time observation of flow-induced cytoskeletal stress in living cells. *Am. J. Physiol. Cell Physiol.* 301:C646–C652, 2011.
- ⁵³Retailleau, K., F. Duprat, M. Arhatte, S. S. Ranade, R. Peyronnet, J. R. Martins, M. Jodar, C. Moro, S. Offermanns, and Y. Feng. Piezo1 in smooth muscle cells is involved in hypertension-dependent arterial remodeling. *Cell Rep.* 13:1161–1171, 2015.
- ⁵⁴Riches, K., P. Warburton, D. J. O'Regan, N. A. Turner, and K. E. Porter. Type 2 diabetes impairs venous, but not arterial smooth muscle cell function: possible role of differential RhoA activity. *Cardiovasc. Revasc. Med.* 15:141–148, 2014.
- ⁵⁵Ritsma, L., S. I. Ellenbroek, A. Zomer, H. J. Snippert, F. J. de Sauvage, B. D. Simons, H. Clevers, and J. van Rheenen. Intestinal crypt homeostasis revealed at single-stem-cell level by in vivo live imaging. *Nature* 507:362, 2014.
- ⁵⁶Schwartz, M. W., R. J. Seeley, M. H. Tschöp, S. C. Woods, G. J. Morton, M. G. Myers, and D. D'aleccio. Cooperation between brain and islet in glucose homeostasis and diabetes. *Nature* 503:59, 2013.
- ⁵⁷Shao, Y., J. M. Mann, W. Chen, and J. Fu. Global architecture of the F-actin cytoskeleton regulates cell shape-dependent endothelial mechanotransduction. *Integr. Biol.* 6:300–311, 2014.
- ⁵⁸Shyu, K.-G. Cellular and molecular effects of mechanical stretch on vascular cells and cardiac myocytes. *Clin. Sci.* 116:377–389, 2009.
- ⁵⁹Sukharev, S., M. Betanzos, C.-S. Chiang, and H. R. Guy. The gating mechanism of the large mechanosensitive channel MscL. *Nature* 409:720, 2001.
- ⁶⁰Sun, Z., S. S. Guo, and R. Fässler. Integrin-mediated mechanotransduction. *J. Cell Biol.* 215:445–456, 2016.
- ⁶¹Topal, T., X. Hong, X. Xue, Z. Fan, N. Kanetkar, J. T. Nguyen, J. Fu, C. X. Deng, and P. H. Krebsbach. Acoustic tweezing cytometry induces rapid initiation of human embryonic stem cell differentiation. *Sci. Rep.* 8:12977, 2018.
- ⁶²Waddingham, M. T., A. J. Edgley, H. Tsuchimochi, D. J. Kelly, M. Shirai, and J. T. Pearson. Contractile apparatus

- dysfunction early in the pathophysiology of diabetic cardiomyopathy. *World J. Diabetes* 6:943, 2015.
- ⁶³Wang, Y., E. L. Botvinick, Y. Zhao, M. W. Berns, S. Usami, R. Y. Tsien, and S. Chien. Visualizing the mechanical activation of Src. *Nature* 434:1040, 2005.
- ⁶⁴Wang, Y., J. Y.-J. Shyy, and S. Chien. Fluorescence proteins, live-cell imaging, and mechanobiology: seeing is believing. *Annu. Rev. Biomed. Eng.* 10:1–38, 2008.
- ⁶⁵Wang, Y., and N. Wang. FRET and mechanobiology. *Integr. Biol.* 1:565–573, 2009.
- ⁶⁶Webster, K. D., W. P. Ng, and D. A. Fletcher. Tensional homeostasis in single fibroblasts. *Biophys. J.* 107:146–155, 2014.
- ⁶⁷Weng, S., Y. Shao, W. Chen, and J. Fu. Mechanosensitive subcellular rheostasis drives emergent single-cell mechanical homeostasis. *Nat. Mater.* 15:961, 2016.
- ⁶⁸Xue, X., X. Hong, Z. Li, C. X. Deng, and J. Fu. Acoustic tweezing cytometry enhances osteogenesis of human mesenchymal stem cells through cytoskeletal contractility and YAP activation. *Biomaterials* 134:22–30, 2017.
- ⁶⁹Xue, X., Y. Sun, A. M. Resto-Irizarry, Y. Yuan, K. M. A. Yong, Y. Zheng, S. Weng, Y. Shao, Y. Chai, and L. Studer. Mechanics-guided embryonic patterning of neuroectoderm tissue from human pluripotent stem cells. *Nat. Mater.* 17:633–641, 2018.
- ⁷⁰Yang, M. T., J. Fu, Y.-K. Wang, R. A. Desai, and C. S. Chen. Assaying stem cell mechanobiology on microfabricated elastomeric substrates with geometrically modulated rigidity. *Nat. Protoc.* 6:187, 2011.
- ⁷¹Yang, M. T., D. H. Reich, and C. S. Chen. Measurement and analysis of traction force dynamics in response to vasoactive agonists. *Integr. Biol.* 3:663–674, 2011.
- ⁷²Zhang, Y., A. Gordon, W. Qian, and W. Chen. Engineering nanoscale stem cell niche: Direct stem cell behavior at cell–matrix interface. *Adv. Healthc. Mater.* 4:1900–1914, 2015.

Publisher's Note Springer Nature remains neutral with regard to jurisdictional claims in published maps and institutional affiliations.